# Supporting Information

# Tuning the photocurrent responsive and resistive switching performances of stilbazolium/iodoargentate hybrids by modulating aggregation mode among chromophores

Jing-Jing Chen[a,b], Chang-Qi Huang[a,b], Hong-Mei Yi[c], Zhou-Lin Lv[c], Wei Wu[c], Hui-Dong Zheng*[a,b] and Hao-Hong Li*[c]

[a] *Fujian Engineering Research Center of Advanced Manufacturing Technology for Fine Chemicals, College of Chemical Engineering, Fuzhou University, Fuzhou, Fujian, 350108, China*

[b] *Qingyuan Innovation Laboratory, Quanzhou, Fujian, 362801, China*

[c] *College of Chemistry, Fuzhou University, Fuzhou, Fujian, 350108, China*

**Table S1** Crystal data and structure refinement for in this work.

| | **1** | **2** | **3** |
|---|---|---|---|
| Empirical formula | $C_{18}H_{20}Ag_2I_3N_3$ | $C_{17}H_{21}Ag_2I_3N_2O$ | $C_{36}H_{46}Ag_5I_7N_4O_4$ |
| Formula weight | 874.81 | 865.80 | 2026.42 |
| Crystal system | Monoclinic | Monoclinic | Triclinic |
| Space group | $P2_1/n$ | $P2_1/c$ | $P$-1 |
| a [Å] | 16.053(3) | 7.1992(4) | 8.1248(7) |
| b [Å] | 7.0422(14) | 13.5373(8) | 13.8287(12) |
| c [Å] | 21.680(4) | 22.6977(14) | 22.9897(19) |
| α[°] | 90 | 90 | 100.297(2) |
| β[°] | 107.705(3) | 90.1810(10) | 93.606(2) |
| γ[°] | 90 | 90 | 103.612(2) |
| Volume [$Å^3$] | 2334.9(8) | 2212.1(2) | 2455.1(4) |
| Z | 4 | 4 | 2 |
| Density (calculated) [$mg/m^3$] | 2.489 | 2.600 | 2.741 |
| Absorption coefficient [$mm^{-1}$] | 5.652 | 5.965 | 6.400 |
| F(000) | 1608 | 1592 | 1856 |
| Theta range for data collection [°] | 1.97 to 25.08 | 1.794 to 25.355 | 1.546 to 25.088 |
| Reflections collected | 14049 | 17991 | 19675 |
| Independent reflections | 4147[$R$(int)= 0.0223] | 4037[$R$(int) = 0.0220] | 8589 [$R$(int) = 0.0329] |
| Data / restraints / parameters | 4147 / 0 / 237 | 4037 / 1 / 234 | 8589 / 6 / 528 |
| Goodness-of-fit on $F^2$ | 1.065 | 1.180 | 1.058 |
| Final R indices [I>2sigma(I)] | $R_1$ = 0.0382, w$R_2$ = 0.0851 | $R_1$ = 0.0426, w$R_2$ = 0.1131 | $R_1$ = 0.0401, w$R_2$ = 0.0902 |
| Largest diff. peak and hole [$e \cdot Å^{-3}$] | 1.223 and -1.217 | 1.655 and -0.971 | 1.705 and -1.583 |

**Table S2** Selected bond lengths (Å) and angles of **1** and **2**.

| **1** | | | | | |
|---|---|---|---|---|---|
| Ag(1)-I(1) | 2.8148(8) | Ag(1)-I(2) | 2.9859(9) | Ag(1)-I(3) | 2.7711(9) |
| Ag(1)-I(2)#1 | 2.9378(9) | Ag(2)-I(1) | 2.8259(9) | Ag(2)-I(2)#1 | 2.9417(9) |
| Ag(2)-I(2)#2 | 2.9986(9) | Ag(2)-I(3)#2 | 2.7872(9) | Ag(1)-Ag(1)#1 | 3.1319(13) |
| Ag(2)-Ag(2)#3 | 3.3123(14) | | | | |
| I(3)-Ag(1)-I(1) | 116.09(3) | I(3)-Ag(1)-I(2)#1 | 114.54(3) | I(1)-Ag(1)-I(2)#1 | 102.25(3) |
| I(1)-Ag(1)-I(2) | 100.35(2) | I(3)-Ag(1)-I(2) | 106.86(3) | I(2)#1-Ag(1)-I(2) | 116.17(2) |
| I(3)#2-Ag(2)-I(1) | 121.40(3) | I(3)#2-Ag(2)-I(2)#1 | 109.95(3) | I(1)-Ag(2)-I(2)#1 | 101.89(3) |
| I(1)-Ag(2)-I(2)#2 | 105.29(3) | I(2)#1-Ag(2)-I(2)#2 | 112.23(2) | I(3)#2-Ag(2)-I(2)#2 | 106.10(3) |
| Symmetry codes: #1 -x+2,-y+2,-z; #2 x,y-1,z; #3 -x+2,-y+1,-z | | | | | |
| **2** | | | | | |
| Ag(1)-I(1) | 2.8150(10) | Ag(1)-I(2) | 2.9505(10) | Ag(1)-I(3) | 2.7876(10) |
| Ag(1)-I(2)#1 | 2.9233(10) | Ag(2)-I(1)#3 | 2.8061(10) | Ag(2)-I(2) | 2.9540(11) |
| Ag(2)-I(2)#2 | 2.9271(10) | Ag(2)-I(3) | 2.7834(10) | Ag(1)-Ag(1)#1 | 3.1778(17) |
| Ag(2)-Ag(2)#2 | 3.2458(18) | | | | |
| I(1)-Ag(1)-I(2)#1 | 102.93(3) | I(1)-Ag(1)-I(2) | 109.26(3) | I(2)#1-Ag(1)-I(2) | 114.50(3) |
| I(3)-Ag(1)-I(1) | 115.63(3) | I(3)-Ag(1)-I(2) | 101.33(3) | I(3)-Ag(1)-I(2)#1 | 113.60(3) |
| I(1)#3-Ag(2)-I(2)#2 | 103.05(3) | I(1)#3-Ag(2)-I(2) | 110.16(3) | I(2)#2-Ag(2)-I(2) | 113.01(3) |
| I(3)-Ag(2)-I(1)#3 | 117.16(4) | I(3)-Ag(2)-I(2)#2 | 112.50(3) | I(3)-Ag(2)-I(2) | 101.34(3) |
| Symmetry codes: #1 -x,-y+1,-z+1; #2 -x+1,-y+1,-z+1; #3 x+1,y,z | | | | | |

**Table S3** Selected bond lengths (Å) and angles of **3**.

| | | | | | |
|---|---|---|---|---|---|
| Ag(1)-I(1) | 2.8593(9) | Ag(1)-I(2) | 2.8320(8) | Ag(1)-I(3) | 2.8521(10) |
| Ag(1)-I(5)#1 | 2.8479(9) | Ag(2)-I(1) | 2.8646(9) | Ag(2)-I(2) | 2.8676(9) |
| Ag(2)-I(4) | 2.7937(8) | Ag(2)-I(6) | 2.9744(9) | Ag(3)-I(4) | 2.7978(9) |
| Ag(3)-I(1)#2 | 2.8673(9) | Ag(3)-I(5) | 2.8803(9) | Ag(3)-I(6) | 2.9724(9) |
| Ag(4)-I(3)#2 | 2.9058(11) | Ag(4)-I(5) | 2.8419(10) | Ag(4)-I(6) | 3.0200(9) |
| Ag(4)-I(7) | 2.7923(9) | Ag(5)-I(2) | 2.8779(10) | Ag(5)-I(3) | 2.8442(10) |
| Ag(5)-I(6) | 2.9482(9) | Ag(5)-I(7) | 2.8136(10) | Ag(1)-Ag(2) | 2.9563(9) |
| Ag(1)-Ag(3)#1 | 2.9799(10) | Ag(1)-Ag(4)#1 | 2.9922(10) | Ag(1)-Ag(5) | 3.0488(10) |
| Ag(2)-Ag(3) | 3.1488(10) | Ag(2)-Ag(5) | 3.2346(10) | Ag(3)-Ag(4) | 3.1235(10) |
| Ag(4)-Ag(5) | 3.1639(11) | | | | |
| I(2)-Ag(1)-I(5)#1 | 97.79(3) | I(2)-Ag(1)-I(3) | 112.35(3) | I(5)#1-Ag(1)-I(3) | 114.96(3) |
| I(2)-Ag(1)-I(1) | 115.06(3) | I(5)#1-Ag(1)-I(1) | 112.82(3) | I(3)-Ag(1)-I(1) | 104.31(3) |
| I(4)-Ag(2)-I(1) | 109.31(3) | I(4)-Ag(2)-I(2) | 114.62(3) | I(1)-Ag(2)-I(2) | 113.79(3) |
| I(4)-Ag(2)-I(6) | 103.37(3) | I(1)-Ag(2)-I(6) | 109.69(3) | I(2)-Ag(2)-I(6) | 105.39(3) |
| I(4)-Ag(3)-I(1)#2 | 109.65(3) | I(4)-Ag(3)-I(5) | 112.86(3) | I(1)#2-Ag(3)-I(5) | 111.61(3) |
| I(4)-Ag(3)-I(6) | 103.32(3) | I(1)#2-Ag(3)-I(6) | 108.18(3) | I(5)-Ag(3)-I(6) | 110.82(3) |
| I(7)-Ag(4)-I(5) | 124.29(3) | I(7)-Ag(4)-I(3)#2 | 105.14(3) | I(5)-Ag(4)-I(3)#2 | 113.48(3) |
| I(7)-Ag(4)-I(6) | 99.24(3) | I(5)-Ag(4)-I(6) | 110.53(3) | I(3)#2-Ag(4)-I(6) | 100.96(3) |
| I(7)-Ag(5)-I(3) | 115.15(3) | I(7)-Ag(5)-I(2) | 113.82(3) | I(3)-Ag(5)-I(2) | 111.22(3) |
| I(7)-Ag(5)-I(6) | 100.47(3) | I(3)-Ag(5)-I(6) | 109.29(3) | I(2)-Ag(5)-I(6) | 105.81(3) |

Symmetry codes: #1 x+1,y,z; #2 x-1,y,z

**Table S4** Hydrogen bridging details of this work.

| Compound | D–H···A | D–H/Å | H···A/Å | D···A/Å | ∠(D–H···A)/° | Symmetry codes |
|---|---|---|---|---|---|---|
| **1** | C(1)-H(1B)···I(1) | 0.98 | 2.97 | 3.916(7) | 161 | x,1+y,z |
| | C(1)-H(1C)···N(3) | 0.98 | 2.64 | 3.225(10) | 118 | |
| **2** | O(1)-H(1)···I(1) | 0.84 | 2.96 | 3.781(14) | 166 | -2-x,2-y,1-z |
| **3** | O(2)-H(2)···O(1) | 0.84 | 1.91 | 2.728(10) | 164 | x,-1+y,z |
| | O(4)-H(4)···O(3) | 0.84 | 2.19 | 2.752(15) | 125 | -1+x,-1+y,z |
| | C(20)-(20B)···O(4) | 0.99 | 2.24 | 3.197(16) | 163 | 1-x,2-y,-z |
| | C(30)-H(30)···I(1) | 0.95 | 3.05 | 3.909(9) | 152 | x,1+y,z |
| | C(36)-(36A)···I(3) | 0.99 | 2.85 | 3.50(3) | 124 | |

**Table S5** π–π stacking interactions in this work (lengths in Å and angles in °).

| | Cg(I)···Cg(J) | Symmetry code | Dist. Centroids | Dihedral angle | CgI_Perp dist. | CgJ_Perp dist. |
|---|---|---|---|---|---|---|
| **2** | Cg(1)→Cg(2) | 1+x,y,z | 3.781(8) | 10.3(7) | 3.171(5) | 3.486(6) |
| | Ring(1):N(1)→C(2)→C(3)→C(4)→C(5)→C(6)→;Ring(2):C(9)→C(10)→C(11)→C(12)→C(13)→C(14)→ | | | | | |
| **3** | Cg(1)→Cg(2) | 2-x,2-y,-z | 3.874(5) | 8.2(4) | 3.338(4) | 3.540(4) |
| | Cg(3)→Cg(4) | -1-x,1-y,1-z | 3.853(5) | 1.6(4) | 3.552(3) | 3.588(4) |
| | Ring(1):C(28)→C(29)→C(30)→C(31)→C(32)→C(33)→;Ring(2):N(3)→C(21)→C(22)→C(23)→C(24)→C(25)→ | | | | | |
| | Ring(3):C(10)→C(11)→C(12)→C(13)→C(14)→C(15)→;Ring(4):N(1)→C(3)→C(4)→C(5)→C(6)→C(7)→ | | | | | |

**Table S6** The excited and emission peaks for hybrids and their organic chromophores.

| Compound | Excited peaks (nm) | Emission peaks (nm) | Shift amount (nm) |
|---|---|---|---|
| CMAMP·I | 585 | 641 | 51 |
| **1** | 551 | 590 | |
| HMAMP·I | 601 | 661 | 6 |
| **2** | 605 | 667 | |
| HMAHP·I | 355 | 734 | 53 |
| **3** | 617 | 681 | |

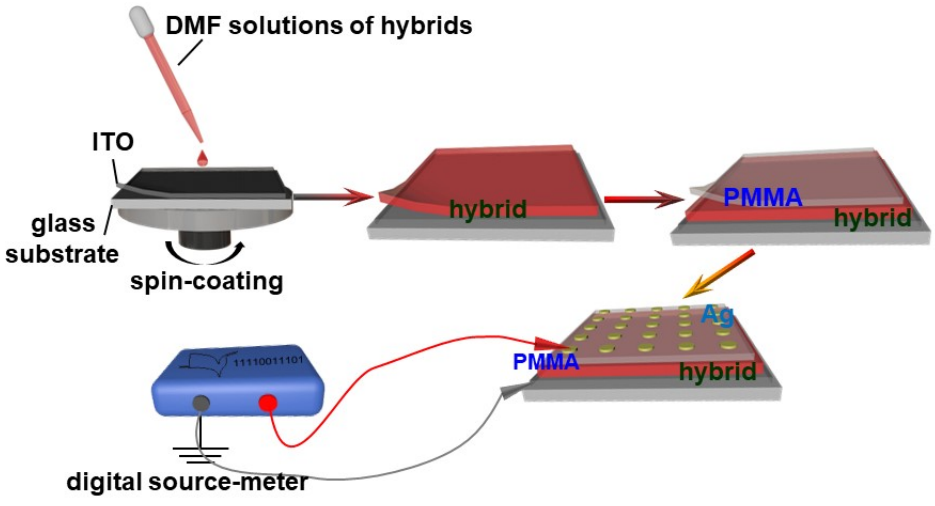


**Scheme S1** The preparing process of ITO/hybrid/PMMA/Ag memory devices.

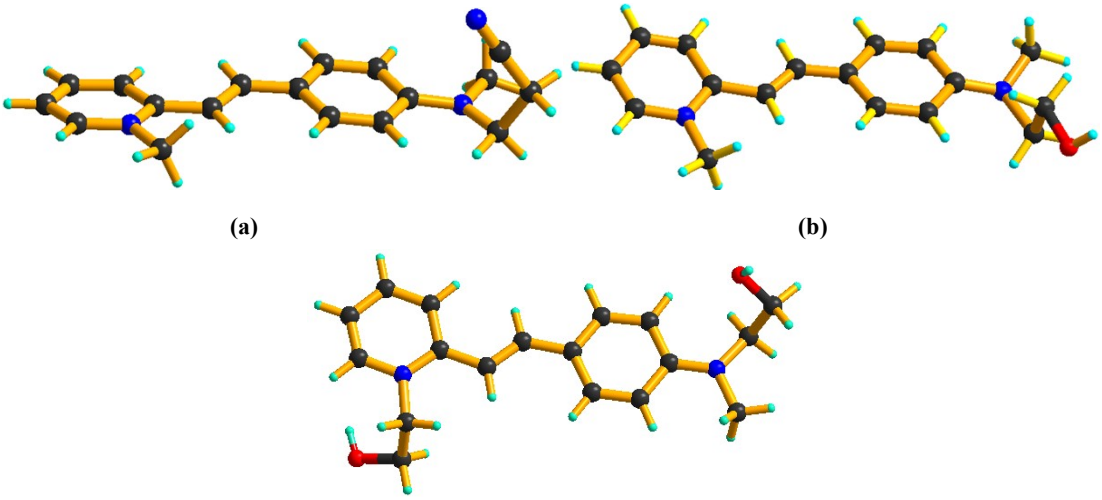

**(a)** **(b)**

**(c)**

**Fig. S1** The conformations of three stilbazolium cations: (a) $CMAMP^+$; (b) $HMAMP^+$; (c) $HMAHP^+$

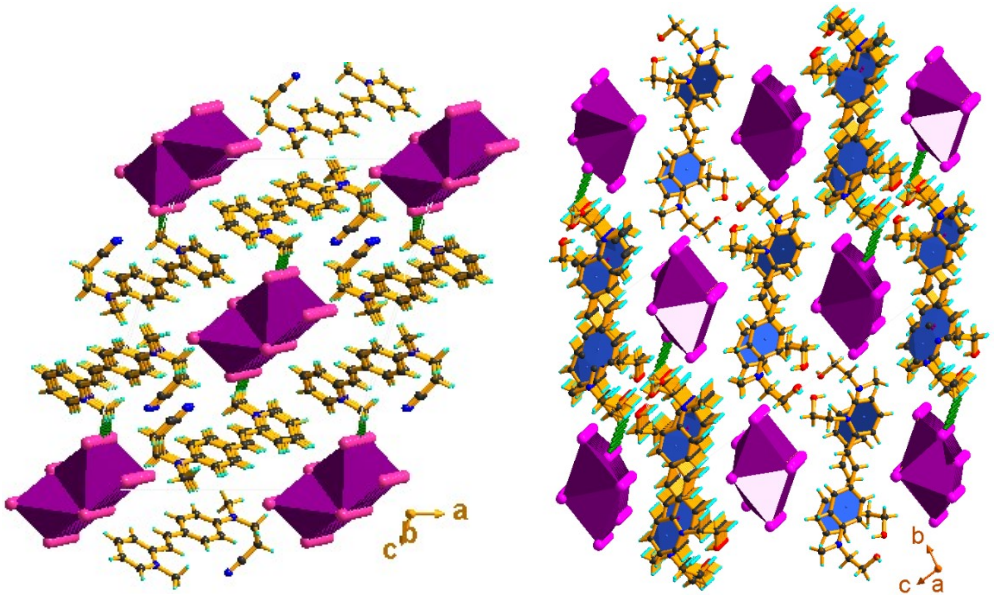


**(a)** **(b)**

**Fig. S2** Packing diagrams showing the quantum-well architectures: (a) $[(CMAMP)(Ag_2I_3)]_n$; (b) $[(HMAHP)_2(Ag_5I_7)]_n$

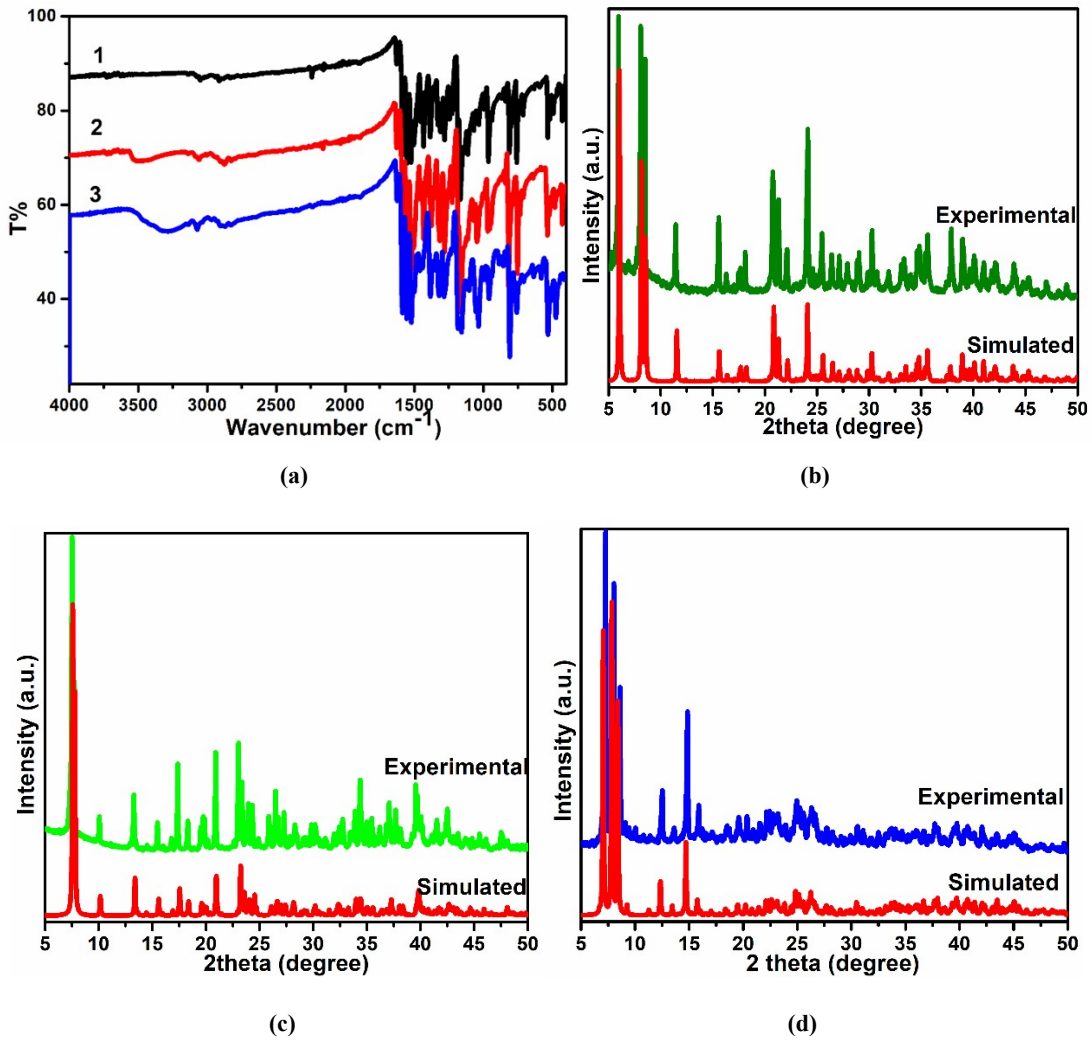


**Fig. S3** (a) FT-IR spectra of **1**~**3**; PXRD patterns: (b) **1**; (c) **2**; (d) **3**

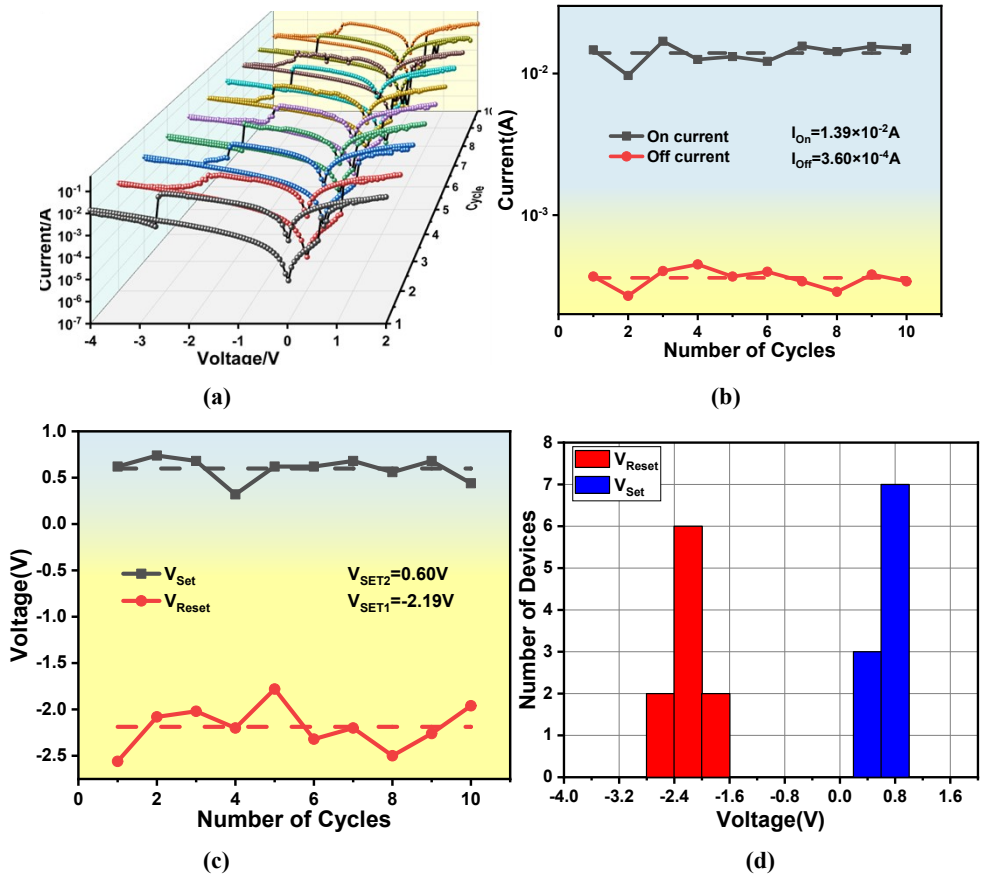


**Fig. S4.** Binary WORM resistive switching performance of ITO/hybrid **2**/Ag device: (a) *I*-*V* characteristics showing 6 cycles; (b) ON/OFF currents with 6 cycles; (c) $V_{Set}$ and $V_{Reset}$ with 6 cycles; (d) $V_{Set}$ and $V_{Reset}$ distributions

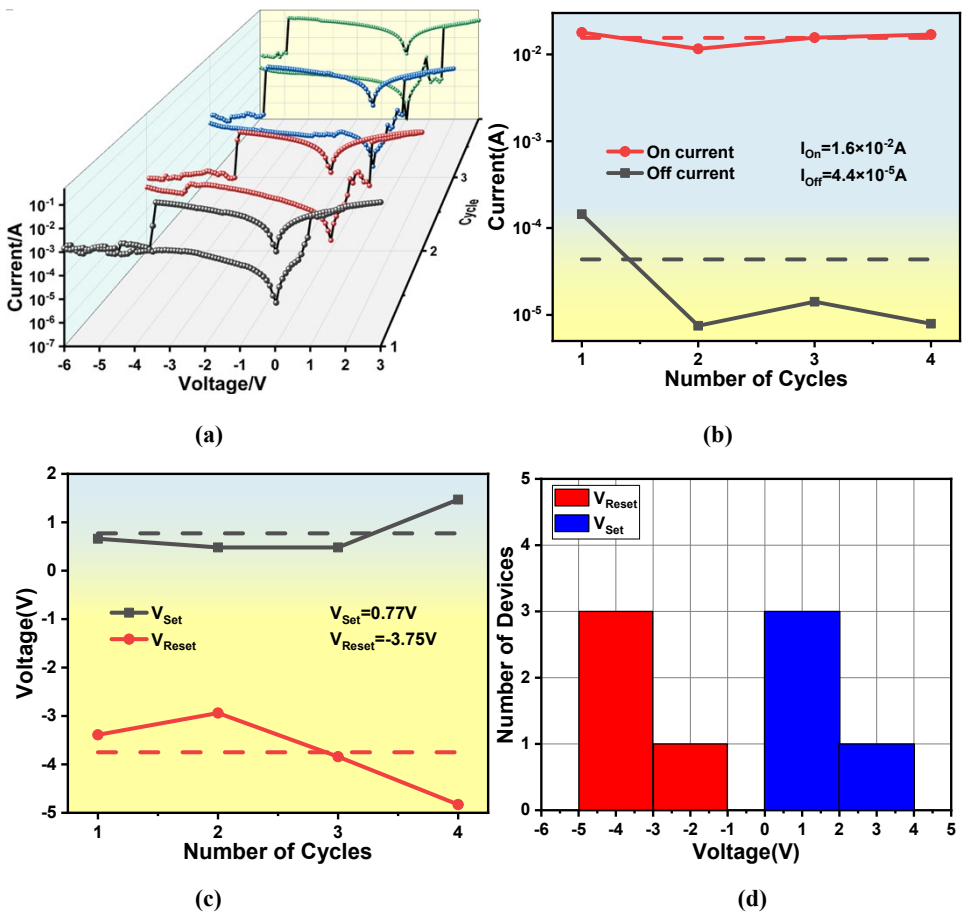


**Fig. S5** Binary WORM resistive switching performance of ITO/hybrid **3**/Ag device: (a) *I*-*V* characteristics showing 6 cycles; (b) ON/OFF currents with 6 cycles; (c) $V_{Set}$ and $V_{Reset}$ with 6 cycles; (d) $V_{Set}$ and $V_{Reset}$ distributions.

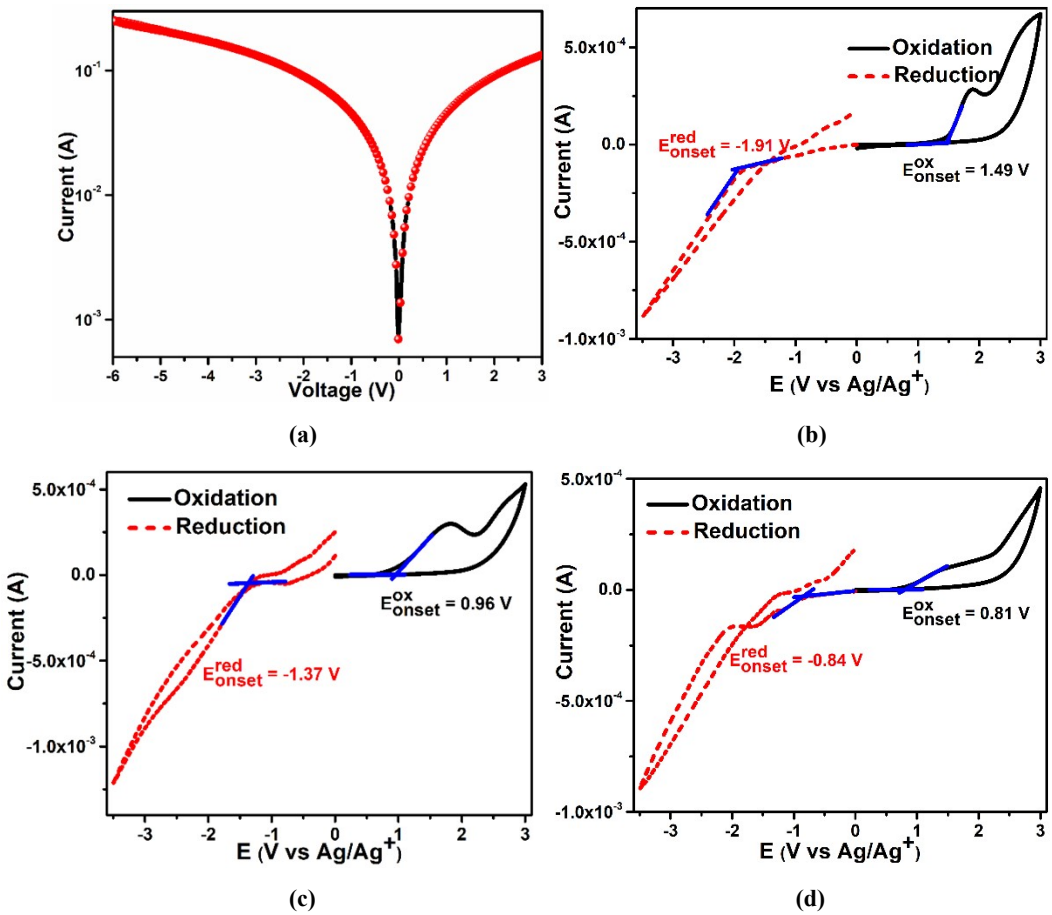


**Fig. S6** (a) *I-V* characteristics curves of ITO/hybrid **3**/Ag device; CV measurements: (b) **1**; (c) **2**; (d) **3**.

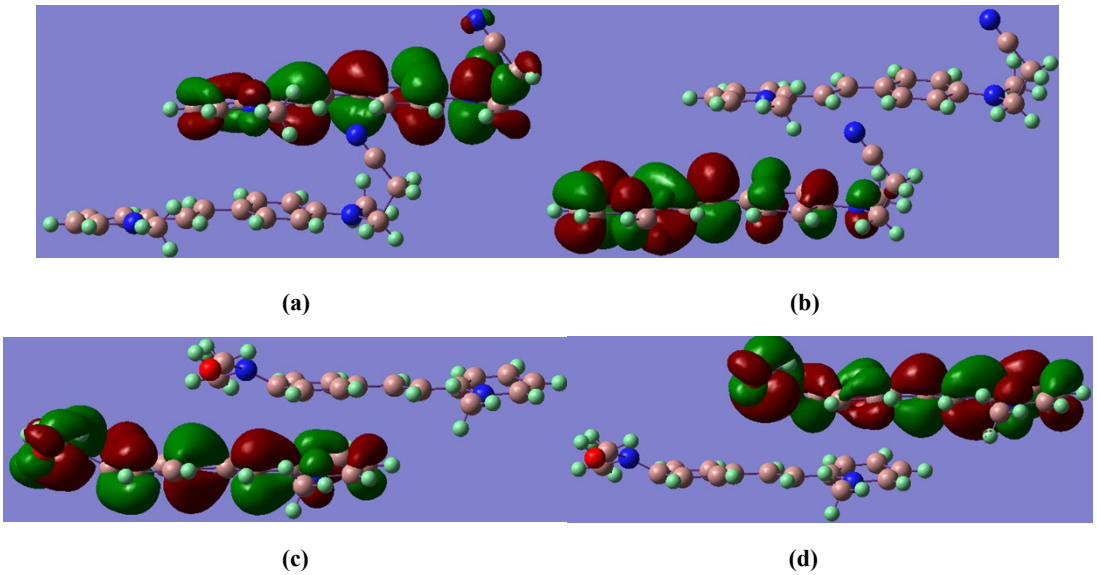


**Fig. S7** Frontier molecular orbitals: (a) HOMO (a) and LUMO of $(CMAMP)_2^{2+}$ dimer in **1**; (c) HOMO (d) and LUMO of $(HMAMP)_2^{2+}$ dimer in **2**.